# Magnetoresistance in thin palladium-carbon mixture films

A. Carl, G. Dumpich, and D. Hallfarth
*Tieftemperaturphysik, Universität Duisburg, 4100 Duisburg 1, Federal Republic of Germany*
(Received 8 March 1988; revised manuscript received 2 September 1988)

We report magnetoresistance measurements on thin granular $Pd_xC_{1-x}$ films with various compositions ($0.45 < x < 1$) which have been prepared by codeposition of pure palladium and high-purity carbon onto quartz crystal substrates at room temperature. The localization-induced magnetoresistance is found to be positive for all $Pd_xC_{1-x}$ films investigated, which gives evidence of the presence of strong spin-orbit coupling. Electron-electron interaction effects on the resistance behavior are also observed, but only in high magnetic fields ($B > 3$ T). The phase-breaking time $\tau_\Phi$ is obtained from the magnetoresistance measurements for temperatures between 1.7 and 20 K, showing a power-law dependence with $p = 1$ below 5 K and with $p = 2$ above. For temperatures $T > 20$ K the inelastic scattering time $\tau_i$ is found to be proportional to $T^{-3}$ ($T^{-1}$ at high temperatures) as revealed by the $R_\square(T)$ behavior of the various $Pd_xC_{1-x}$ films. We find that $\tau_\Phi$ coincides with $\tau_i$ at appropriate temperatures, which experimentally proves that $\tau_i(T)$ is a continuously varying function in the whole temperature range ($1.7 < T < 300$ K) investigated. The results are compared with theoretical predictions as well as with recent measurements on pure Pd and Pd-Au films by other authors.

## I. INTRODUCTION

It is well established that the low-temperature behavior of the resistance of thin metallic films is influenced by weak localization (WL) and/or electron-electron interactions (EEI's).[1,2] Both effects lead to additional contributions to the Boltzmann resistance ($R_B$) which can be well explained by the theoretical predictions.[3–5] Moreover, it has been shown in the past several years that fitting the experimental data by the theoretical expressions allows one to determine various electron scattering times, e.g., for inelastic, spin-orbit, and magnetic scattering processes.[6] Since the determination of the various scattering times is essentially based on theoretical predictions, the scattering rates are sometimes regarded as being fit parameters only. On the other hand, it is argued that there are some restrictions on the values from other (independent) experiments which allow one to confirm a reliable determination of the scattering times, at least for experiments in two dimensions (2D).[7] E.g., the temperature dependence of the inelastic scattering rate $\tau_i$ seems for a large number of materials[8–12] to vary as $\tau_i \sim T^{-p}$ with $p = 1$ for temperatures $T < 4.2$ K and with $p$ between 2 and 3 for temperatures above $T = 4.2$ K. However, the absolute values of $\tau_i$ and its physical interpretation are still topics of controversial discussions.[13] In some cases good agreement between experimental results and recent theories can be achieved (e.g., Refs. 13–16). On the other hand, it is found that the scattering times may depend on the film resistance,[17] the film thickness,[18] and film structure.[19]

Generally thin films of various resistances (using the same material) are produced by changing the condensation conditions (e.g., substrate temperature, evaporation rate, evaporation time). Due to the different nucleation and growth processes during condensation the film structure or even its topology can also be changed, leading to holes, cracks, or channels in thin films.[20] This results in quite different electron scattering situations which give rise to variations of the scattering rates by 1 order of magnitude.[17] Thus, to study systematically the behavior of the scattering rates, those systems should be favorable which are expected to allow variations of the resistance (disorder), without changing their structural properties.

As for investigations of the metal-insulator transition,[21] we propose to use metal-insulator mixtures for studying the resistance behavior of thin films in view of weak localization effects. We have chosen Pd-C mixtures, since carbon is known to be insoluble into palladium. Palladium carbides have not been observed.[22] On the other hand, recent studies of the magnetoresistance of thin Pd (Pd-Au) films give very useful information for our present investigation in the sense of a standard.[13,23–25] In this paper we report magnetoresistance measurements of thin *metallic* $Pd_xC_{1-x}$ mixture films far above the percolation threshold. TEM investigations reveal that the $Pd_xC_{1-x}$ films form well-connected Pd clusters, their overall structural properties being essentially the same, if the carbon content is less than about 50%. We find that the residual resistivity of the mixture films continuously increases with increasing carbon content. From the temperature dependence of the resistance ($T > 50$ K) the inelastic electron mean free path is obtained. Magnetoresistance measurements provide the inelastic scattering rates at low temperatures. The temperature dependence of the scattering times for all the $Pd_xC_{1-x}$ films investigated display the same general features. It exhibits a continuously varying function of the scattering time as obtained from the magnetoresistance measurements in line with those (independently) obtained from the "high"-temperature resistance behavior. We conclude that the existence of a crossover for the inelastic scatter-

 

ing time, as revealed for all samples investigated, gives an additional check for the quantitative determination of the scattering times.

## II. EXPERIMENT

Thin $Pd_xC_{1-x}$ mixture films of various composition $x$ are prepared by codeposition of pure palladium (less than 1 ppm magnetic impurity concentration) and high-purity carbon onto quartz-crystal substrates at room temperature in an UHV system. During deposition the system pressure is kept below $p=1\times10^{-7}$ mbar. Palladium is evaporated by electron-beam heating of a bulk Pd pellet, carbon is sublimated from a thin carbon rod by resistance heating. Using different ratios of the evaporation rates for Pd (C) various films of different Pd concentrations $x$ with $0<x<1$ are prepared. The deposition of carbon and palladium is independently monitored by two separate quartz crystal oscillators, both calibrated by optical interferometry (Tolansky). From this the composition $x$ and the total film thickness $t$ has been determined ranging between 10–70 nm for the various $Pd_xC_{1-x}$ films.

In each run three $Pd_xC_{1-x}$ films with fixed composition are deposited simultaneously onto quartz- and NaCl-crystal substrates. The different substrates are precoated by carbon to yield similar condensation conditions for deposition. The three samples are used for resistance measurements, x-ray analysis, and TEM analysis, respectively. The temperature dependence of the resistance is measured *in situ* for substrate temperatures between 3 and 300 K by means of an UHV $^4$He-gasflow cryostate. The film resistance is measured by means of four terminal dc technique with a resolution of $\Delta R/R\approx10^{-5}$; measuring currents were chosen between 10 and 100 $\mu$A to avoid sample heating.

The magnetoresistance (MR) measurements were carried out in a separate $^4$He cryostate ($1.7<T<300$ K), where magnetic fields up to 5 T can be applied. Within the accuracy limits no difference in the temperature dependence of the resistance is found, although the samples are exposed to air when using the second setup.

## III. RESULTS

$Pd_xC_{1-x}$ thin films are invesitgated in the whole concentration region ($0<x<1$) as prepared. In the present paper we concentrate on the temperature and field dependence of the resistance for films with compositions ($0.45<x<1$) well above the percolation threshold $x_p=0.3$. Figure 1 shows electron micrographs of a "pure" Pd film (a) and a $Pd_xC_{1-x}$ mixture film with $x=0.45$ (b). The thickness of the films are $t=38.4$ and 25.7 nm respectively. As one can see from the micrographs, the films consist of well-connected small Pd grains (dark) with mean diameters of about $\Phi=6$ nm. The mean cluster sizes as well as the cluster-size distributions $P(\Phi)$ are found to be almost the same for the different films in Fig. 1. On the other hand, the films contain holes and channellike structures, the number and size of which increase when adding carbon. This results from the presence of carbon which prohibits a complete coalescence of the growing Pd clusters during condensation and leads to the formation of bottlenecklike connections between the Pd clusters. Looking more precisely at the two micrographs one recognizes that the contact areas between the clusters are smaller for the mixture film (b) as compared to the pure Pd film (a). This shows that carbon acts as a filling factor only. The overall film topology, as, e.g., shown in Fig. 1, is found to be very similar for all the $Pd_xC_{1-x}$ films investigated within $0.45<x<1$.

The mean lattice parameter $\bar{a}=0.395$ nm, as determined from diffraction patterns taken from the same films as in Fig. 1, is close to the bulk value $a_b=0.389$ nm of pure Pd. Analyzing x-ray diffraction patterns taken from the various $Pd_xC_{1-x}$ films we find the lattice parameter to be independent of the carbon content. Since a solubility of carbon in palladium has not been observed,[22] the dilation of carbon into the Pd clusters is not very likely. In fact, a detailed analysis of the lattice parameter by means of electron diffraction using a reference method confirms this idea.[26]

$Pd_xC_{1-x}$ films with compositions well above the percolation threshold ($x>x_p$) show metallic resistance be-

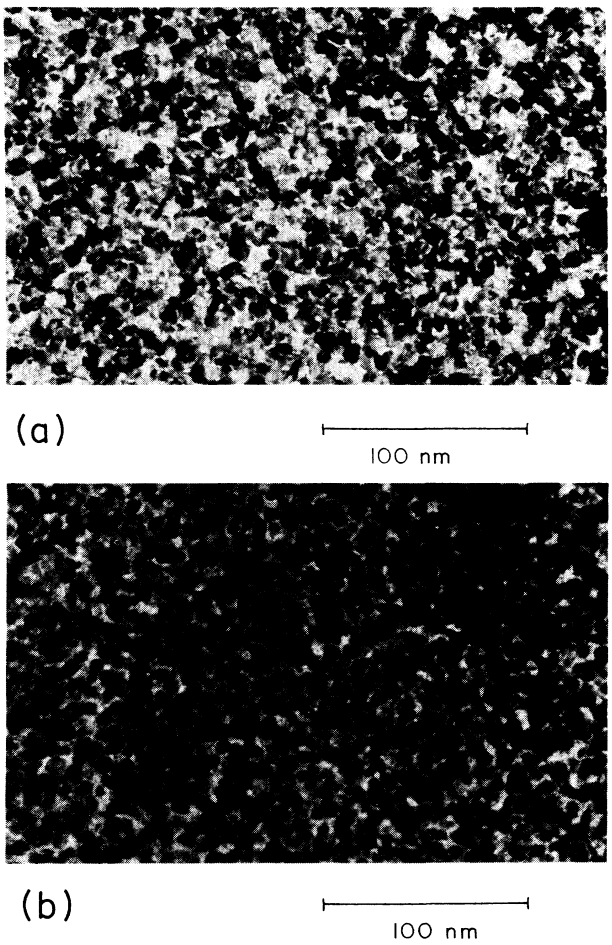


FIG. 1. Electron micrographs for a pure palladium film (a) and a $Pd_{0.45}C_{0.55}$ film (b) with thicknesses $t=38.4$ and 25.7 nm.

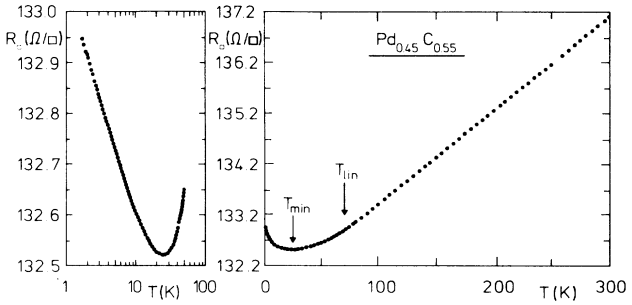


FIG. 2. Resistance/□ vs temperature in a linear (right) and half-logarithmic (left) presentation for a $Pd_{0.45}C_{0.55}$ film.

havior as revealed by the linear temperature dependence of the resistance. This is typically shown in the right-hand side of Fig. 2, where the resistance per square $R_\square$ for the $Pd_{0.45}C_{0.55}$ film is plotted versus the temperature $T$. As one can see from Fig. 2 the resistance linearly decreases from room temperature down to about $T_{\rm lin}=72$ K. At low temperatures the resistance exhibits a minimum at $T_{\rm min}=25$ K and shows a logarithmic increase for temperatures $T<T_{\log}$ (left-hand side of Fig. 2). The occurrence of a resistance minimum with a logarithmic temperature dependence for $T<T_{\log}$ has been observed for the whole series of $Pd_xC_{1-x}$ thin films with compositions above the percolation threshold. The relevant data are given in Table I. Figure 3 shows the normalized magnetoresistance which is given by

$$\delta\sigma(B)\equiv-[R_\square(T,B)-R_\square(T,0)]/[R_\square(T,0)]^2$$

versus log$B$ as measured for various fixed temperatures. The different symbols in each graph denote the experimental MR data as obtained at different temperatures between 2.1–21 K. The solid lines are calculated using the theoretical predictions, as will be discussed in Sec. IV. As one can see from Fig. 3 the overall MR behavior for the different $Pd_xC_{1-x}$ films is independent of the composition of the films. For each temperature one finds the MR to increase with increasing magnetic field (positive MR). There is no indication for a maximum in the MR even for fields up to 4.5 T. Due to the limits of accuracy in determining the MR of our samples we find the MR to start up at magnetic fields $B\approx10^{-2}$ T. For fields between $10^{-2}$ and 0.5 T the MR weakly increases and (for temperatures below 8 K) it shows a logarithmic field dependence above $B=1$ T. When the temperature is raised, $\delta\sigma(B)$ decreases for (fixed) magnetic fields. As one can see from Fig. 3, the MR data of the various $Pd_xC_{1-x}$ films differ from each other only by their absolute values.

## IV. ANALYSIS

From the residual resistance of the $Pd_xC_{1-x}$ films we obtain the mean free path $l_e$ for elastic electron scattering. Following Drude's law $l_e$ is simply given by

$$l_e=[(1.27\times10^4\ \Omega)n^{-2/3}]\sigma_R^\infty$$

with $n$ the electron density and $1/\sigma_R^\infty$ the residual resistivity for films with (in principle) infinite thickness. According to Fuchs-Sontheimer (FS) theory one expects the resistivity for thin films to depend on the thickness.[27] Thus we measured the thickness dependence of the resistance for the different $Pd_xC_{1-x}$ films during condensation. Plotting $1/\sigma_R$ versus thickness $t$ we find for the present $Pd_xC_{1-x}$ films that the resistivity is constant for thicknesses larger than 10 nm. Since the actual thicknesses of our $Pd_xC_{1-x}$ films are larger than at least 25 nm, size effects can be neglected, i.e., $1/\sigma_R$ ($t>10$ nm)$=1/\sigma_R^\infty$. For the electron density we assume $n=2.45\times10^{28}$ m$^{-3}$ as given by Ref. 28 for the whole set of $Pd_xC_{1-x}$ films investigated. Using Drude's law we find (see Table I) $l_e=2.07$, 1.5, 1.03, and 0.45 nm for Pd concentrations $x=1$, 0.8, 0.65, and 0.45 of the $Pd_xC_{1-x}$ films, respectively. There are several sources of errors when determining absolute values of $l_e$ from the residual resistivity due to the structure of the films as can be seen in Fig. 1 and to the uncertainty obtaining the effective masses of electrons and holes in Pd (two-band model). However, relative changes of $l_e$ with concentration for the various $Pd_xC_{1-x}$ films can be determined quite accurately, since the effective masses and the density of electrons should be independent on details of the granular structure of the films. In fact, we find the mean elastic scattering length $l_e$ as calculated above to linearly decrease with decreasing Pd concentration $x$. Moreover, plotting $l_e$ versus $\Gamma$, the residual resistance ratio $\Gamma=R_\square(300\ {\rm K})/R_\square(4.2\ {\rm K})$, we find $l_e$ linearly to decrease with decreasing $\Gamma$, i.e., with increasing disorder. Using Matthiessen's law, the linear correlation $l_e\sim\Gamma$ is rather expected, since $l_e=(\Gamma-1)l_i(300\ {\rm K})$, where $l_i(300\ {\rm K})$ is the inelastic electron mean free path at 300 K. This experimentally proves that Matthiessen's law ($l_\infty^{-1}=l_e^{-1}+l_i^{-1}$) can be applied for the present analysis. Furthermore, it confirms that the values for $l_e$ as determined from the residual resistance of the various $Pd_xC_{1-x}$ mixture films appear to be correct, at least rela-

TABLE I. Data on a series of $Pd_xC_{1-x}$ thin films with compositions above the percolation threshold.

| $x$ (at. %) | $t$ (nm) | $R_\square^{\rm min}$ (Ω/□) | $\Gamma$ | $l_e$ (nm) | $k_Fl_e$ | $\delta\sigma(T)$ (mho □) $10^{-5}$ | $T_{\rm lin}$ (K) | $T_{\log}$ (K) |
|---|---|---|---|---|---|---|---|---|
| 1 | 38.4 | 19.41 | 1.31 | 2.07 | 18.6 | 0.3 | 45 | 3.5 |
| 0.8 | 26.1 | 39.26 | 1.23 | 1.5 | 13.5 | 1.0 | 63 | 5.0 |
| 0.65 | 68.1 | 21.71 | 1.11 | 1.03 | 9.3 | 2.4 | 62 | 7.0 |
| 0.45 | 25.7 | 132.52 | 1.04 | 0.45 | 4.0 | 2.6 | 72 | 9.0 |

tively among each other. Using Matthiessen's law we calculate the inelastic scattering length $l_i$ for each temperature between $T_{\text{lin}}$ and 300 K. Due to the linear temperature dependence of the resistance (Fig. 2), this consequently yields a simple power-law temperature dependence of $l_i$ with $l_i \sim T^{-1}$. For temperatures $T$ between $T_{\text{min}}$ and $T_{\text{lin}}$ we found—using a $R_\square$ versus $T^3$ presentation—$l_i$ essentially to vary as $T^{-3}$. In the vicinity of $T_{\text{min}}$ and $T_{\text{lin}}$, $l_i(T)$ shows a $T^{-2}$ dependence. The temperature dependence of the inelastic scattering times $\tau_i(T)=l_i(T)/v_F$ with $v_F=5.3\times10^5$ m/s (Ref. 23) as obtained from the $R_\square(T)$ curves between 20 and 300 K is shown by the solid lines in Figs. 4(a)–4(d). For the $T^{-3}$ dependence of $\tau_i(T)$ between $T_{\text{min}}$ and $T_{\text{lin}}$ see the inset in Fig. 4(a).

The magneotresistance as shown in Fig. 3 exhibits only positive contributions. There are no indications for a maximum in the MR even at higher magnetic fields. That means—within the framework of 2D localization—that the MR's of the $Pd_xC_{1-x}$ films are strongly influenced by spin-orbit scattering processes.[29] In this case, $\delta\sigma(B)$, the normalized magnetoresistance, is given by

$$\delta\sigma(B)=-\alpha_B\frac{e^2}{2\pi^2\hbar}\left[\ln\frac{B_\Phi}{B}-\psi\left[\frac{1}{2}+\frac{B_\Phi}{B}\right]\right]. \quad (1)$$

Here $\psi(x)$ is the digamma function, $B$ is the applied magnetic field, $B_\Phi=B_i(T)+2B_s$, and $B_i, B_s$ are characteristic fields according to inelastic and magnetic scattering processes, respectively. The prefactor $\alpha_B$ is constant and should be $\alpha_B=-0.5$ (Ref. 29). The use of Eq. (1) implies that the characteristic field for spin-orbit scattering $B_{\text{s.o.}}$ is much larger than $B_i$ and $B_s$ (see Ref. 29). In fact, if $B_{\text{s.o.}}$ would be only slightly larger than $B_\Phi$, $\delta\sigma(B)$ is expected to exhibit a maximum for magnetic fields $B>B_{\text{s.o.}}$, which is not observed for the present $Pd_xC_{1-x}$ films. This means that $B_{\text{s.o.}}$ should be at least larger than $B=5$ T, the maximum magnetic field which can be applied in our case. A more careful analysis shows that, when using the full theoretical expression for the $MR$ as given in Ref. 29, $\delta\sigma(B)$ is identical with the values obtained from Eq. (1) if $B_{\text{s.o.}}>8$ T, justifying the use of Eq. (1) for the present analysis.

$B_i(T)$ and $B_s$ can be expressed in terms of corresponding relaxation times $\tau_i(T)$ and $\tau_s$ with

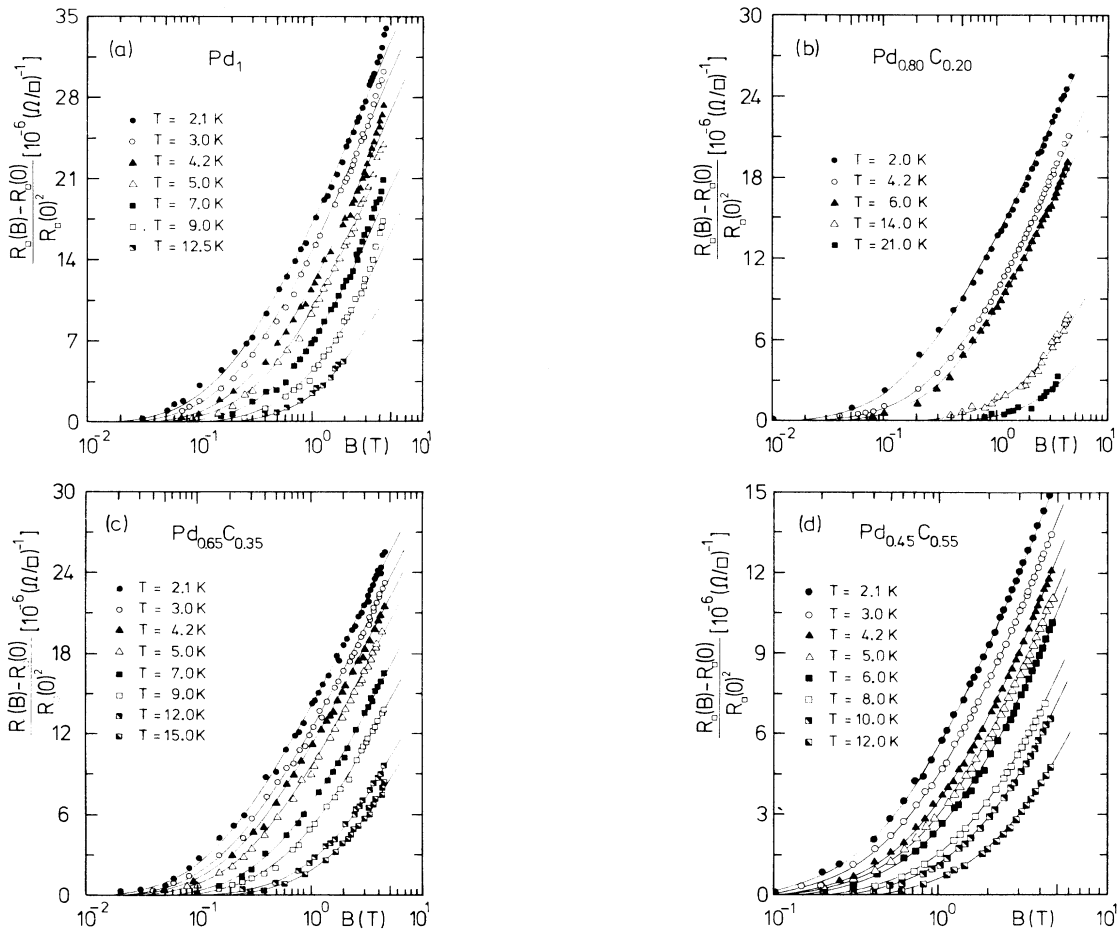


FIG. 3. Magnetoresistance curves for $Pd_xC_{1-x}$ films with compositions $0.45<x<1$ at various temperatures. The solid lines are due to a fit from Eq. (1).

$$\tau_i(T)=\frac{\hbar}{4DeB_i(T)} \text{ and } \tau_s=\frac{\hbar}{4DeB_s} , \quad (1a)$$

while $D=v_F l_e/3$ is the diffusion constant. With $l_e$, which can be determined by the residual resistivity (see above) and $\alpha_B=-0.5$, there is only one parameter in Eq. (1) remaining ($B_\Phi$) to fit $\delta\sigma(B)$ to the experimental data given in Fig. 3. This one-parameter fitting process yields good agreement between theory [Eq. (1)] and the experimental data (Fig. 3) for all investigated $Pd_xC_{1-x}$ films up to magnetic fields of about $B=2.5$ T. For magnetic fields $B>3$ T we find $\delta\sigma(B)$ at 4.2 K systematically to be about 10% smaller than the experimental data in Fig. 3. This could be due to an additional contribution to the magnetoresistance based on EEI's which are known to be not negligible for high magnetic fields.[30] The lowest limit for the occurrence of a reliable logarithmic contribution based on EEI's in the MR in 2D is given by $B_{e\text{-}e}=\mu_0 k_B T/g\mu_B$. With $g=2$ and $T=4.2$ K we find $B_{e\text{-}e}=3.1$ T, which shows that MR contributions from Coulomb interactions have to be taken into account at least for magnetic fields $B>3$ T. Calculating $\delta\sigma(B)$ in case of Coulomb interactions at high magnetic fields with $\tau_{s.o.}\ll\tau_i$ we make use of[30]

$$\delta\sigma(B)=-\frac{e^2}{4\pi^2\hbar}(1+F)\ln\left[\frac{g\mu_B B}{\mu_0 k_B T}\right] . \quad (2)$$

With $F=0.74$ as calculated from the free-electron model, this leads to an additional logarithmic MR contribution above 3.1 T, which is of the same order of magnitude as found for the deviations between experimental data and theory based solely on localization [Eq. (1)]. Thus, assuming that Coulomb interactions as well as localization effects are simply additive, quantitative agreement between experiment and theory can be well achieved. Since Coulomb interactions only cause a small contribution to the MR in the low-field limit with $\delta\sigma(B)\sim B^2$, we used a different fit process for the present analysis. Disregarding Coulomb contributions—only for simplicity—we assume $\alpha_B$ to be a "second" fit parameter in Eq. (1). It

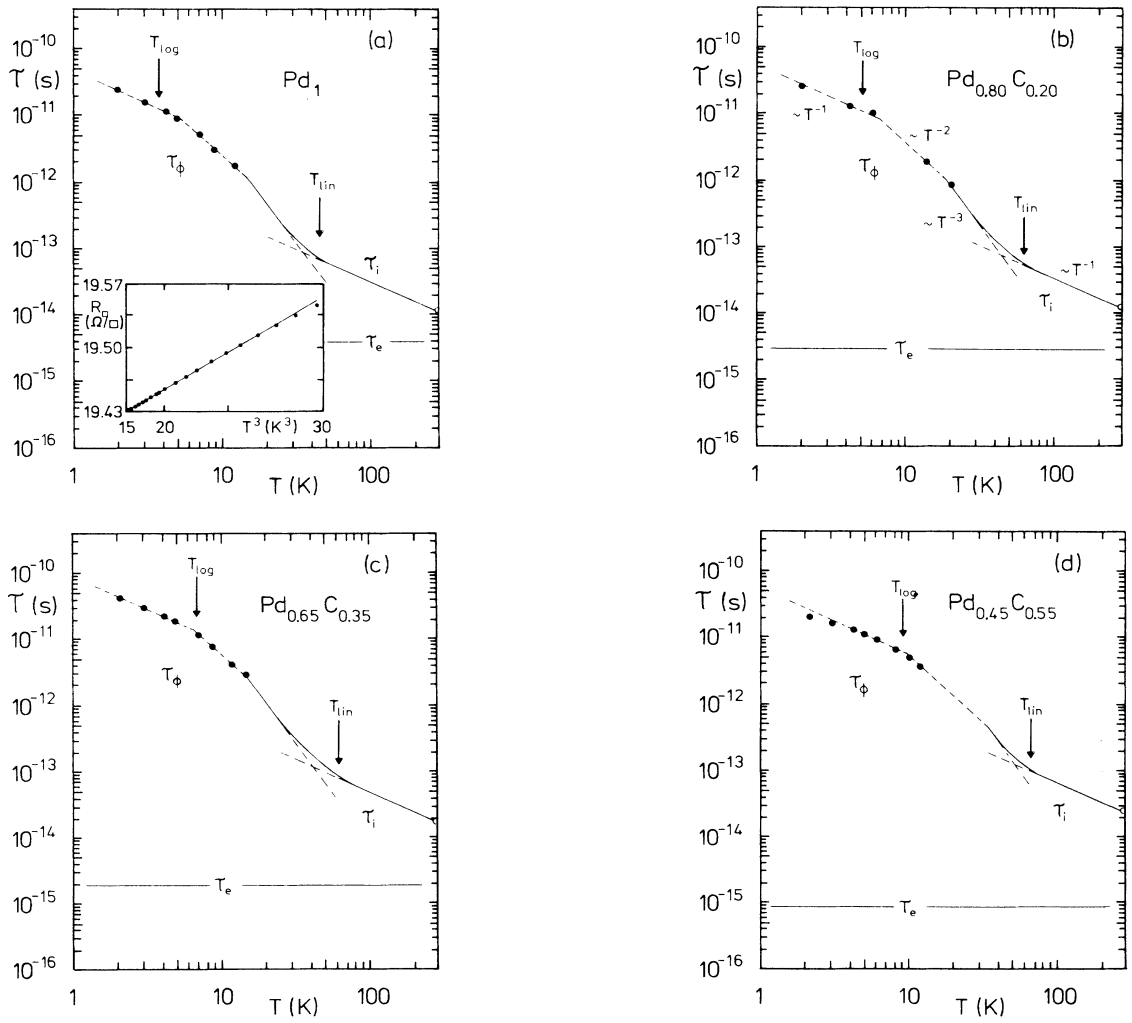


FIG. 4. log-log presentation of the scattering times $\tau_\Phi$, $\tau_i$, and $\tau_e$ vs temperature for different $Pd_xC_{1-x}$ films with compositions $0.45<x<1$. Dashed lines indicate $T^{-1}$, $T^{-2}$, and $T^{-3}$ behavior of $\tau_\Phi, \tau_i$.

turns out—as one can see by the solid lines in Fig. 3—that $\alpha_B = -0.65$ yields an excellent fit to the experimental data in Fig. 3 between 1.8 and 20 K and for magnetic fields up to 4.5 T for all $Pd_xC_{1-x}$ films. From this fit we obtain $B_\Phi$ as a function of temperature for the various $Pd_xC_{1-x}$ films. Using Eq. (1a) this gives the phase coherence time $\tau_\Phi(T)$ as shown in Fig. 4 (solid dots). We emphasize that the values of $\tau_\Phi$ are almost equal, independent if either $\alpha_B = -0.5$ or $\alpha_B = -0.65$ is used for the fit. The data $\tau_\Phi$ are given in Figs. 4(a)–4(d) by the solid dots. Dashed lines are only guides to the eye, indicating the $T^{-1}$, $T^{-2}$, and $T^{-3}$ behavior of the scattering times.

## V. DISCUSSION

As one can typically see from Fig. 4(a) the phase coherence time $\tau_\Phi$ varies for temperatures $T < T_{\log}$ linearly with the inverse of the temperature ($\tau_\Phi \sim T^{-1}$) followed by a $T^{-2}$ dependence for $T > T_{\log}$. This behavior has been observed for all $Pd_xC_{1-x}$ mixture films [see the various data in Figs. 4(a)–4(d)] with carbon concentrations up to about 35%. For higher carbon contents (see $Pd_{0.45}C_{0.55}$), $\tau_\Phi(T)$ deviates upwards the linear temperature dependence at low temperatures ($T < 5$ K) which will be discussed below.

The absolute value of $\tau_\Phi = 8.65 \times 10^{-12}$ s at low temperatures (e.g., at $T = 5$ K) agrees well with those recently obtained from other MR measurements for (pure) Pd thin films.[23,24] Markiewicz *et al.*[23] found $\tau_\Phi$ ranging from $7.55 \times 10^{-12}$ to $1.51 \times 10^{-11}$ s, depending on the film resistance, and McGinnis *et al.*[24] obtained $\tau_\Phi = 4.55 \times 10^{-12}$ s.

Recently, Lin and Giordano discussed the temperature dependence of electron scattering times from weak localization of Au-Pd films.[7,13] They found—in line with others[31]—the inelastic scattering rate to linearly increase with decreasing temperature for $T < 5$ K as to result from electron-electron scattering.

Taking into account strong momentum dependence of the phase coherence time $\tau_\Phi$, as done by Altshuler *et al.* (AAK),[32] $\tau_\Phi$ is given by

$$\left[\frac{1}{\tau_\Phi}\right]_{ee}^{\mathrm{AAK}} = \frac{e^2 R_\Box}{2\pi\hbar^2} k_B T \ln\left[\frac{\pi\hbar}{e^2 R_\Box}\right], \tag{3}$$

exhibiting a $\tau_\Phi \sim T^{-1}$ behavior at low temperatures. Calculating $\tau_\Phi$ by Eq. (3) yields $(\tau_\Phi)_{ee}^{\mathrm{AAK}} = 3.13 \times 10^{-10}$ s for the $Pd_1$ film at $T = 5$ K, which is about a factor of 36 larger than the experimental value given in Table II. Since the deviation from the theoretical value is far above the experimental uncertainties, it seems to indicate that the magnitude of $\tau_\Phi$ is not consistent with the theory. For evaporated Au-Pd thin films, Lin and Giordano[13] also found $(\tau_\Phi)_{\mathrm{expt}}$ by more than an order of magnitude smaller than predicted, whereas for sputtered Au-Pd films $\tau_\Phi$ agrees well with the theory. As pointed out, this discrepancy is not yet understood.

TABLE II. Data for $Pd_xC_{1-x}$ thin films.

| $x$ (at. %) | $\tau_\Phi^{\mathrm{expt}}$ ($T=5$ K) ($10^{-11}$ s) | $\tau_{ee}^{\mathrm{AAK}}$ ($T=5$ K) ($10^{-11}$ s) | $\tau_{e\text{-ph}}^{\mathrm{3D}}$ ($T=5$ K) ($10^{-11}$ s) |
|---|---|---|---|
| 1 | 0.865 | 31.3 | 141 |
| 0.8 | 1.0 | 17.4 | 102 |
| 0.65 | 1.85 | 28.5 | 70 |
| 0.45 | 1.06 | 6.5 | 30.6 |

According to Eq. (3), $(\tau_\Phi)_{ee}^{\mathrm{AAK}}$ decreases with increasing resistance. As one can see from Table II, $(\tau_\Phi)_{ee}^{\mathrm{AAK}}$ becomes around six times larger than $(\tau_\Phi)_{\mathrm{expt}}$ for the $Pd_{0.45}C_{0.55}$ film. Thus we find for the films with higher resistance better agreement between the theoretically predicted values [Eq. (3)] and the experimental data. Previously, Bergmann,[33] and, recently, Lin and Giordano, pointed out that the inelastic scattering rate due to electron-electron scattering (2D) in the presence of disorder appears better to describe the experimental results obtained from the high-resistivity ($k_F l_e > 1$) thin films rather than from the "clean" films ($k_F l_e \gg 1$), in agreement with our results. As mentioned above the temperature dependence of $\tau_\Phi(T)$ becomes weaker than $\tau_\Phi \sim T^{-1}$ for films with higher carbon concentration ($Pd_{0.45}C_{0.55}$). Moreover, we find $\tau_\Phi$ to saturate for films approaching the percolation threshold (not shown). This behavior has also been observed by other authors who investigated the MR of thin films of various materials.[14–16] It has been proposed that the saturation behavior of $\tau_\Phi$ may result from magnetic scattering processes even if the magnetic impurity concentration is small ($\approx 1$ ppm).[24] If we assume magnetic scattering processes to be dominant at low tempeatures it follows that from Eq. (1) $B_\Phi \approx 2B_s$. Thus extrapolating the experimental values of $\tau_\Phi$ for the $Pd_{0.45}C_{0.55}$ film to $T = 1$ K assuming $\tau_\Phi \approx$ const, we find $\tau_\Phi(1\ \mathrm{K}) = 2 \times 10^{-11}$ s and with $\tau_s = 2\tau_\Phi$ at $T = 1$ K, $\tau_s = 4 \times 10^{-11}$ s. Compared to, e.g., $\tau_s = 7.36 \times 10^{-12}$ s, as obtained by recent measurements for a 55-Å Pd film,[23] the values of $\tau_s$ for the present $Pd_xC_{1-x}$ films are even larger, which means that even less magnetic scattering processes should be involved in our films.

For temperatures $T_{\log} < T < 20$ K the various graphs in Fig. 4 consistently show that $\tau_\Phi(T)$ varies with $\tau_\Phi \sim T^{-2}$. This has been found for a large number of materials.[5,34] It has been discussed that electron-phonon interactions in the presence of impurities lead to a temperature dependence of the inelastic scattering time $\tau_i$ with $\tau_i \sim T^{-2}$ in 3D. Calculating the phonon wavelength $\lambda_{\mathrm{ph}} = 12.6$ nm for the most probable acoustic phonon wave number $q_T = 2k_B T/\hbar v_s$ with $v_s = 2.63 \times 10^3$ m/s, the speed of sound,[24] we find for $T = 5$ K, $l_e < \lambda_{\mathrm{ph}}$ and $t > \lambda_{\mathrm{ph}}$ ($t \approx 30$ nm) valid for all samples investigated. Thus, with respect to electron-phonon interaction, they can be treated as to be in the dirty 3D case. In this case the inelastic scattering rate in 3D is given by[35]

$$\left[\frac{1}{\tau_i}\right]_{e\text{-ph}}^{\mathrm{3D}} = 2\pi^2 \frac{a}{k_F l_e} \frac{k_B T^2}{\hbar \Theta_D}, \tag{4}$$

where

$$a = \frac{m^* n}{6\rho_M} \left[\frac{k_B \Theta_D}{\hbar k_F} \frac{v_F}{v_s^2}\right]^2 .$$

With $\rho_M = 12.16 \times 10^3$ kg/m$^3$ the mass density for Pd,[24] we obtain $(\tau_i)^{3D}_{e\text{-ph}} = 1.41 \times 10^{-9}$ s at $T = 5$ K, which is about a factor of 160 larger than the experimental value for $Pd_1$. As one can see from Fig. 4 we find—in accordance with the behavior of $(\tau_i)^{AAK}_{ee}$—the theoretically predicted values of $(\tau_i)^{3D}_{e\text{-ph}}$ to agree better with the experimental data for films with higher disorder. But also in this case (see the data for the $Pd_{0.45}C_{0.55}$ film in Fig. 4) the theoretical value for $(\tau_i)^{3D}_{e\text{-ph}} = 3.06 \times 10^{-10}$ s at $T = 5$ K is about a factor of 30 larger than the experimental value. This more clearly demonstrates, as for the values of $(\tau_i)^{AAK}_{ee}$, that a comparison of the *absolute* values of the inelastic scattering times with the experimental data is still problematic, whereas the temperature dependence of the scattering times is found to be in good agreement with the experimental results.

One of the most interesting features of the $\tau_\Phi(T)$ behavior (Fig. 4) is the fact, that extrapolating $\tau_\Phi \sim T^{-2}$ to higher temperatures, $\tau_\Phi$ continuously joins the inelastic scattering time $\tau_i$ as determined from the $R_\square(T)$ curves. This means, that although $\tau_\Phi$ and $\tau_i$ are determined from completely different experimental situations, $\tau_\Phi(T), \tau_i(T)$ exhibit a continuously varying function of temperature between 2 and 300 K. We emphasize that $\tau_\Phi = \hbar/4eDB_\Phi$ is obtained using Eq. (1a), whereas $\tau_i$ is determined from the temperature dependence of the resistivity with $\tau_i = [\tau_e/(\Gamma - 1)]T^{-p}$. Since $\Gamma$ and $B_\Phi(T)$ are fixed parameters as determined from the experimental data, there is only *one* parameter, namely, $\tau_e$, which "adjusts" $\tau_\Phi$ as well as $\tau_i$ in absolute magnitude. If we assume $\tau_e$ to be a fit parameter, variations of $\tau_e$ would lead to variations of $\tau_i$ proportional to $\tau_e$, whereas $\tau_\Phi$ changes inversely proportional to $\tau_e$. Consequently the $\tau_\Phi(T)$ curve shifts down (up), whereas $\tau_i(T)$ increases (decreases) if $\tau_e$ increases (decreases). In these cases the $\tau_\Phi(T)$ curve does not link the $\tau_i(T)$ curve in the appropriate temperature range $T_{\min} < T < 300$ K. Thus there is only *one* unique value for $\tau_e$ which yields $\tau_\Phi(T_c) = \tau_i(T_c)$ at a "crossover" temperature $T_c$. Consistently, this confirms that $\tau_e$ has been determined correctly. Furthermore, it gives experimental evidence that $\tau_\Phi(T)$ as determined from MR measurements is in line identical with $\tau_i(T)$ as determined from the "high"-temperature behavior of $R_\square(T)$. Since we find this behavior of $\tau_\Phi(T), \tau_i(T)$ for all the $Pd_xC_{1-x}$ mixture films investigated, we conclude that the inelastic scattering time is a continuously varying function of temperature due to electron-phonon interaction for temperatures between $T_{\log}$ and 300 K.

## VI. CONCLUSIONS

The low-temperature and low-field dependence of the resistance of thin granular $Pd_xC_{1-x}$ films can be well explained with respect to 2D-localization effects. 2D-Coulomb interaction effects are also found to be present at high magnetic fields. The localization-induced magnetoresistance is found to be positive, indicating strong spin-orbit scattering (symplectic case). From the magnetoresistance data we obtain the phase coherence time $\tau_\Phi^{-1}(T) = \tau_i^{-1}(T) + 2\tau_s^{-1}$ at low temperatures. From the temperature dependence of the resistance we deduce the inelastic scattering time $\tau_i(T)$ in the high temperature range $(20 < T < 300$ K). It is found that $\tau_\Phi(T), \tau_i(T)$ exhibit a continuously varying function of temperature with $(\tau_\Phi, \tau_i) \sim T^{-p}$, where $1 \leq p \leq 3$, depending on the temperature range. For $Pd_xC_{1-x}$ mixture films with $x < 0.65$ there is a tendency for a saturation of $\tau_\Phi$ at low temperatures, which is probably due to magnetic scattering, although we find the magnetic impurity concentration for the present samples to be less than 1 ppm. From the occurrence of a crossover of $\tau_\Phi(T)$ with $\tau_i(T)$ at distinct temperatures we conclude that $\tau_\Phi(T)$ as evaluated from magnetoresistance measurements is in line identical with $\tau_i(T)$ as obtained from the linear high-temperature dependence of the resistance.

## ACKNOWLEDGMENTS

The authors are very grateful to E. F. Wassermann for fruitful discussions and valuable advice. This work was supported by the Deutsche Forschungsgemeinschaft (DFG)—physics of anorganic clusters.

[1] E. Abrahams, P. W. Anderson, D. C. Licciardello, and T. V. Ramakrishnan, Phys. Rev. Lett. **42**, 673 (1979).
[2] B. L. Altshuler, A. G. Aronov, and P. A. Lee, Phys. Rev. Lett. **44**, 1288 (1980).
[3] Y. Bruynseraede and M. Gijs, in *Advances in Solid State Physics XXV*, edited by P. Grosse (Vieweg, Braunschweig, 1985), p. 465.
[4] *Anderson Localization*, edited by Y. Nagaoka and H. Fukuyama (Springer, New York, 1982).
[5] *Localization, Interaction and Transport Phenomena*, edited by B. Kramer, G. Bergmann, and Y. Bruynseraede (Springer, New York, 1984).
[6] G. Bergmann, Phys. Rep. **107**, 1 (1984).
[7] J. J. Lin and N. Giordano, Phys. Rev. B **35**, 545 (1987).
[8] G. Deutscher, M. Gijs, C. van Haesendonck, and Y. Bruynseraede, in *Proceedings of the International Conference on Localization, Interaction and Transport Phenomena in Impure Metals*, edited by L. Schweitzer and B. Kramer (Physikalisch-Technische Bundesanstalt, Braunschweig, 1984), Suppl. PTB-PG-1.
[9] F. Komori, S. Kobayashi, and W. Sasaki, J. Phys. Soc. Jpn. **52**, 4306 (1983).
[10] A. C. Sacharoff and R. M. Westervelt, Phys. Rev. B **32**, 662 (1985).
[11] T. Kagwaguti and Y. Fujimori, J. Phys. Soc. Jpn. **52**, 722 (1983).
[12] F. Komori, S. Kobayashi, and W. Sasaki, J. Phys. Soc. Jpn. **52**, 368 (1983).
[13] J. J. Lin and N. Giordano, Phys. Rev. B **35**, 1071 (1987).
[14] C. van Haesendonck, M. Gijs, and Y. Bruynseraede, in Ref. 5.
[15] P. Santhanam and D. E. Prober, Phys. Rev. B **29**, 3733 (1984).
[16] M. Gijs, C. van Haesendonck, and Y. Bruynseraede, J. Phys.

F **16**, 1227 (1986).
[17]R. P. Peters and G. Bergmann, in Ref. 8, pp. 167–170.
[18]P. Chandhari, H. U. Habermeier, and S. Maekawa, Phys. Rev. Lett. **55**, 430 (1985).
[19]G. Dumpich, H. Kristen, and E. F. Wassermann, Z. Phys. B **51**, 251 (1983).
[20]N. T. Liang, Ch. Ki, and Sh. Wang, Solid State Commun. **51**, 385 (1984).
[21]G. Deutscher, in *Percolation, Localization and Superconductivity,* edited by A. M. Goldmann and St. A. Wolf (Plenum, New York, 1984).
[22]F. A. Shunk, *Constitution of Binary Alloys* (McGraw-Hill, New York, 1969).
[23]R. S. Markiewicz and C. J. Rollins, Phys. Rev. B **29**, 735 (1984).
[24]W. C. McGinnis and P. M. Chaikin, Phys. Rev. B **32**, 6319 (1985).
[25]L. Dumoulin, H. Raffy, P. Nedellec, D. S. MacLachlan, and J. P. Burger, Solid State Commun. **51**, 85 (1984).
[26]R. Anton (unpublished).
[27]K. Fuchs, Proc. Cambridge Philos. Soc. **34**, 100 (1938).
[28]M. Gijs, Y. Bruynseraede, and A. Gilabert, Solid State Commun. **57**, 141 (1986).
[29]S. Hikami, A. I. Larkin, and Y. Nagaoka, Prog. Theor. Phys. **63**, 707 (1980).
[30]S. Kobayashi, Ref. 5.
[31]See Ref. 7 and Refs. 49–53 therein.
[32]B. L. Altshuler, in *Electron-Electron Interactions in Disordered Systems,* edited by A. L. Efros and M. Pollak (Elsevier, Amsterdam, 1985), p. 72.
[33]G. Bergmann, Z. Phys. B **48**, 5 (1982).
[34]D. Abraham and R. Rosenbaum, Phys. Rev. B **27**, 1413 (1983).
[35]H. Takayama, Z. Phys. **263**, 329 (1973).

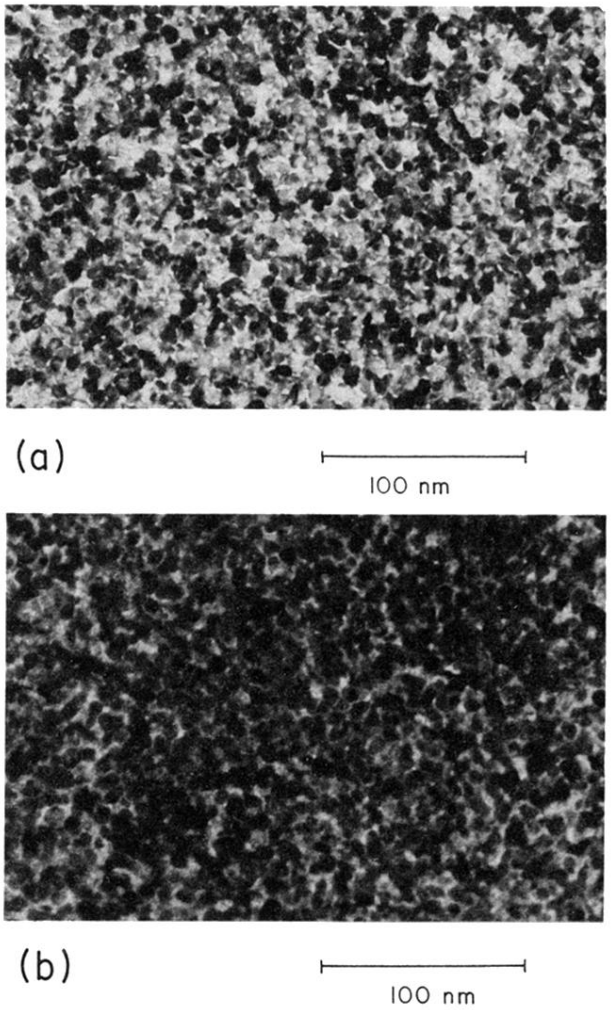


FIG. 1. Electron micrographs for a pure palladium film (a) and a $Pd_{0.45}C_{0.55}$ film (b) with thicknesses $t = 38.4$ and 25.7 nm.